

# Axial-Loaded MRI Using a SpineMAC Device to Show Narrowing of Dural Sac and Disc Height in Lumbar Spinal Stenosis

Witaya Sungkarat, MD, PhD<sup>1,4</sup>, Jiraporn Laothamatas, MD<sup>2</sup>, Ladawan Worapruengkjaru, MSc<sup>3</sup>, Boonthida Hooncharoen, MD<sup>4</sup>, Jarruwat Charoensuk, PhD<sup>5</sup>, Khaisang Chousangsuntorn, DEng<sup>6</sup>

<sup>1</sup> Department of Diagnostic and Therapeutic Radiology, Faculty of Medicine Ramathibodi Hospital, Mahidol University, Bangkok, Thailand

<sup>2</sup> Faculty of Health Sciences Technology, HRH Princess Chulabhorn College of Medical Science, Chulabhorn Royal Academy, Bangkok, Thailand

<sup>3</sup> Division of Radiation Oncology, Department of Diagnostic and Therapeutic Radiology, Faculty of Medicine Ramathibodi Hospital, Mahidol University, Bangkok, Thailand

<sup>4</sup> Advanced Diagnostic Imaging Center (AIMC), Faculty of Medicine Ramathibodi Hospital, Mahidol University, Bangkok, Thailand

<sup>5</sup> Department of Mechanical Engineering, Faculty of Engineering, King Mongkut's Institute of Technology Ladkrabang, Bangkok, Thailand

<sup>6</sup> Department of Radiological Technology, Faculty of Medical Technology, Mahidol University, Phutthamonthon, Nakhon Pathom, Thailand

**Background:** A lumbosacral spinal compression device has been developed by the authors (SpineMAC) to simulate normal weight-bearing by axial-loading of the lumbar spine while the patient is in the supine position.

**Objective:** To investigate the effect of axial loading using a SpineMAC device, on lumbar spine, spinal canal, and spine curvature, in subjects with suspected spinal stenosis.

**Materials and Methods:** The present study was prospective cross-sectional study. Forty-five (21 males and 24 females) consecutive Thai adults underwent unloaded and axial-loaded supine magnetic resonance imaging (MRI) examinations of the lumbosacral spine. Radiographic parameters included cross-sectional area of disc (DA), cross-sectional area of dural sac (DCSA), disc height (DH), anterior to posterior distance of disc (DAP), L1-L3-L5 angle (LA), and lumbar lordosis (LL).

**Results:** During the axial-loaded MRIs, the pathologic features of the lumbar spinal stenosis such as the disc bulging, nerve root compression, narrowing of the spinal canal, and the spinal neural foramina, were frequently observed in L4-L5 and L5-S1. Radiographic parameters differences of more than 5% between unloaded and axial-loaded supine MRIs were observed in DCSA and DH. Narrowing of the dural sac due to axial compression was observed at the L4-L5 level (8.1%), while loss of DH was found at both the L5-S1 (-7.9%) and the L4-L5 (-6.8%) levels. Axial compression only slightly affected the DA and DAP of the intervertebral discs with a difference of 5% or less. Furthermore, it rarely changed the spine curvature (LL and LA) of the subjects, with a difference of 2% or less. LL decreased during axial loading and may not correlate with the findings during normal standing position. Although the authors found greater DA and DAP values in male ( $p < 0.001$ ) and obese ( $p < 0.05$ ) subjects, changes of radiographic parameters with axial loading were otherwise not correlated with sex, age, or body mass index.

**Conclusion:** An axial-loaded MRI, using a SpineMAC device, may be superior to conventional MRI when evaluating narrowing of the dural sac and disc height of patients.

**Keywords:** Lumbar lordosis, Spinal stenosis, Axial loading, Weight bearing, Disc herniation, Low back pain

Received 9 June 2020 | Revised 30 September 2020 | Accepted 7 October 2020

J Med Assoc Thai 2020;103(12):1325-34

Website: <http://www.jmatonline.com>

## Correspondence to:

Chousangsuntorn K.

Department of Radiological Technology, Faculty of Medical Technology, Mahidol University, 999 Phutthamonthon Sai 4 Road, Salaya, Phutthamonthon District, Nakhon Pathom 73170, Thailand.

Phone: +66-2-2011251, Fax: +66-2-2011176

Email: [hemtiwakorn@gmail.com](mailto:hemtiwakorn@gmail.com)

ORCID: 0000-0003-1308-3389

## How to cite this article:

Sungkarat W, Laothamatas J, Worapruengkjaru L, Hooncharoen B, Charoensuk J, Chousangsuntorn K. Axial-Loaded MRI Using a SpineMAC Device to Show Narrowing of Dural Sac and Disc Height in Lumbar Spinal Stenosis. J Med Assoc Thai 2020;103:1325-34.

[doi.org/10.35755/jmedassocthai.2020.12.11525](https://doi.org/10.35755/jmedassocthai.2020.12.11525)

Lumbar spinal stenosis is characterized by the narrowing of the spinal canal and may cause mechanical compression of the spinal nerve roots<sup>(1)</sup>. Clinical symptoms of lumbar spinal stenosis include neurogenic claudication, which is the most common, low back pain, leg pain such as sciatic type, and muscle weakness<sup>(2)</sup>. The symptoms are worsened by lumbar extension and improved with lumbar flexion<sup>(3)</sup>. Upright standing extends the lumbar spine causing a decrease of the dural sac's cross-sectional area (CSA)<sup>(4-6)</sup>. The constriction of the dural sac is exacerbated when patients are standing or walking<sup>(7-10)</sup> and is improved

when they are lying down<sup>(11)</sup>. In addition, gravity on the body when standing compresses the intervertebral discs (IVDs) of the lumbar spine and may displace disc material beyond the IVD disc space<sup>(12)</sup>. This disc herniation can compress the dural sac of the spinal canal lying between the bulging disc anteriorly and the ligamentum flavum posteriorly<sup>(6,13)</sup>. Narrowing may occur in central spinal canal, in the area under the facet joints, or more laterally in the neural foramina<sup>(3)</sup>.

Magnetic resonance imaging (MRI), a non-ionizing and non-invasive diagnostic tool, is conventionally used to evaluate abnormalities of lumbar spine, with patients in the supine position. However, compared with standing position, supine MRIs may underestimate both pathology such as dural sac and nerve root compression, narrowing of spinal neural foramina, disc bulging, ligamentum flavum thickening, and loss of disc height [DH]<sup>(11,14,15)</sup> and disease severity<sup>(11,16-18)</sup>. Recently, standing MRI has been employed to better study pathology of the lumbar spine, particularly in cases of suspected spinal stenosis in which supine MRI is negative<sup>(19)</sup>. However, standing MRI systems are costly and not widely available<sup>(20)</sup>. In addition, the standing MRI is not practical since patients are required to stand without movement to complete the scan. Though a standing MRI is preferable for claustrophobic patients, it is impractical for the elderly and patients with severe symptoms.

Thus, lumbosacral spinal compression devices have been developed to simulate normal weight-bearing by axial-loading the lumbar spine while the patient is in the supine position<sup>(15,16)</sup>. Several studies have compared the effects of axial-loading devices with the observations of conventional supine MRIs<sup>(15,18,20-24)</sup>. These studies suggest that axial loading devices can add valuable information especially in patients with neurogenic claudication, as well as influence the treatment decision plan for degenerative disorders<sup>(18,21)</sup>, increase the specificity of a diagnosis of spinal stenosis<sup>(11,15,23)</sup>, and accurately correlate with clinical severity<sup>(17)</sup>. Specifically, axial-loaded MRIs in patients with lumbar spinal canal stenosis reflect the changes of the dural sac size and position<sup>(11,17,24,25)</sup>, decreases in DH<sup>(22,25)</sup>, and increases in lumbar lordosis<sup>(22,25)</sup>. However, some have reported that axial loading does not have a clinically relevant effect on the morphology of the lumbar spine<sup>(20)</sup>.

In Thailand, neither lumbosacral compression devices nor standing MRIs are widely used for diagnostic imaging of lumbar stenosis patients. To generate axial loading of the lumbar spine during

MRIs performed in the supine position, the authors developed a lumbosacral spinal compression device. The authors utilized it to perform axial-loaded MRIs in adult subjects who had suspected lumbar spinal stenosis. The purpose of the present study was to evaluate whether axial-loaded MRIs demonstrate morphologic changes of IVD, spinal canal, and spine curvature in this patient group when compared with conventional, unloaded, MRI. The findings of those morphologic changes on lumbar spine due to a lumbosacral spinal compression device in other studies have been inconsistent<sup>(20,22,24,25)</sup>.

## Material and Methods

### Inclusion and exclusion criteria

The authors performed a prospective study that enrolled consecutive Thai adults who had clinical symptoms suggestive of spinal stenosis<sup>(2)</sup> between May 2018 and June 2019. No subject had a previous diagnosis of spinal stenosis and none had bone fractures. Weight and height of the subjects were limited to 100 kg and 180 cm due to the constraints of the lumbosacral spinal compression device. The sample size was calculated based on the standard deviation of CSA of dural sac (DCSA) reported in a previous study<sup>(17)</sup>. All subjects gave written informed consent before participating in the present research. The study was performed in accordance with the Declaration of Helsinki and was approved by the Committee on Human Rights related to Research involving Human Volunteers at the Faculty of Medicine, Ramathibodi Hospital (COA No. MURA2019/252).

### Experimental protocol

Subjects were examined with MRIs done in the supine position, unloaded, and with axial loading. Both the unloaded and the axial-loaded MRI examinations were performed with straight knees to simulate a normal upright position<sup>(11)</sup>. The study was performed using a 3.0 Tesla system (Phillips Ingenia, Phillips Healthcare, Best, Netherland) and a total spine coil.

A non-magnetic, SpineMAC lumbosacral spinal compression device (Advanced Diagnostic Imaging Center, Ramathibodi Hospital, Thailand), developed by the authors (under review by the Thai Food and Drug Administration (FDA); patent pending number 1901006901), was used to apply axial compression. The device consisted of a body vest with two straps connected to separate footplates. By tightening or loosening the adjustment knobs on the compression



**Figure 1.** Supine axial-loaded MRI examination.

part, the load was regulated and separately distributed to the legs. The applied load was measured using scales on each strap. All subjects lay on a slip carpet that covered the MRI table to minimize friction forces between the body of the patient and the table during axial loading. The load applied was 50% of body weight<sup>(3,16)</sup> divided between the two footplates (25% of body weight on each foot) and anchored to the body vest (Figure 1). Sagittal and axial, T1 weighted (T1W) and T2 weighted (T2W), turbo spin echo images of the lumbar spine were acquired. Slice thicknesses were 3.0 mm (180 mm field of view [FOV]) for axial images and 4.0 mm (320 mm FOV) for sagittal images. The box for transverse slices was placed parallel to the disc. Total scan time was approximately 40 minutes to examine both unloaded and axial-loaded supine MRIs.

### Radiographic analysis

All images were exported as DICOM files for analysis with Philips Intellispace Portal 5.3 software. Radiographic pathologic features, including disc budging or protrusion, spinal canal stenosis,

narrowing of spinal neural foramina, nerve root compression, loss of DH, and radial bulging of lumbar discs, were visually analyzed by a radiologist (Hooncharoen B).

Quantitative measurement was performed manually on both unloaded and axial-loaded supine MRI studies using a digitized tool. CSA of IVD (DA) and DCSA were measured in axial T2W images (Figure 2A), while DH and distance from anterior to posterior (DAP) of the IVD were measured in sagittal T1W images (Figure 2B). Angle between L1-L3-L5 (LA) and lumbar lordosis (LL) were measured in mid-sagittal slices of T1W images (Figure 2C). To investigate the inter-observer variability of the measurements in the standing and axial-loaded MRIs, radiological parameters were measured by two experienced radiological technologists (Chousangsuntorn K and Worapruengkjaru L) who were blinded to the other's measurements. Interobserver measurements showed excellent correlation (interclass correlation coefficient [ICC] range 0.90 to 0.99). Mean measurements of each radiological parameter from observers 1 and 2 were calculated and used for the analysis in the present study.

### Statistical analysis

Effects on the axial-loaded MRIs were evaluated and compared with those of the conventional supine (unloaded) MRIs. Normal distribution was checked using a Kolmogorov-Smirnov test. For comparisons of radiographic parameters between unloaded and axial-loaded MRIs, the dependent-sample t-test was used for comparison of the means of parameters with

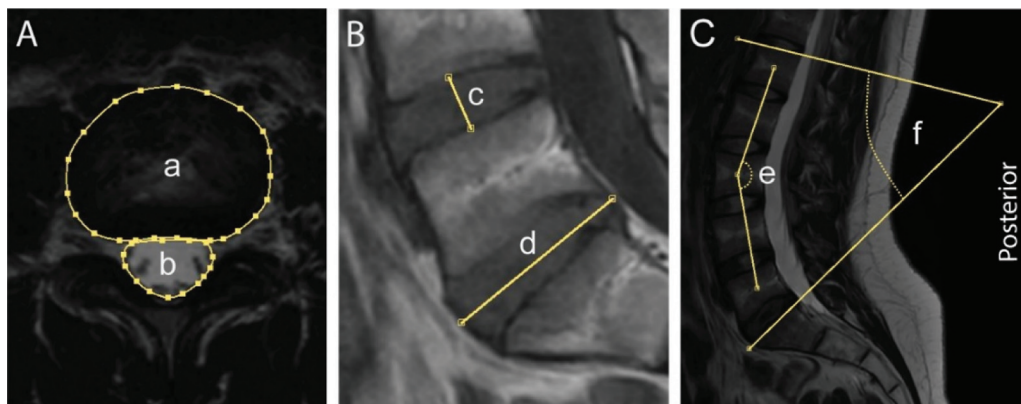


**Figure 2.** Measurements of DA (a) and DCSA (b) in an axial T2W image (A), DH (c) and DAP (d) in a sagittal T1W image (B), and LA (e) and LL (f) in a sagittal T1W image (C). DA, CSA of intervertebral disc; SA, CSA of dural sac; DH, disc height defined by the distance between superior and inferior borders of an IVD exclusive of endplates. DAP, distance between anterior and posterior of edges of a disc at the point of most bulge; LL, angle between superior endplate of L1 and superior endplate of S1; LA, angle of the center of L1-L3-L5.

**Table 1.** Frequency of change of radiographic feature occurring during axial-loaded MRI

MRI feature	Frequency of change; n (%)			
	L2-L3	L3-L4	L4-L5	L5-S1
Disc bulging/protrusion	11 (12.9)	15 (17.7)	31 (36.5)	28 (32.9)
Spinal canal stenosis	6 (10.7)	13 (23.2)	24 (48.9)	13 (23.2)
Narrowing of spinal neural foramina	3 (7.7)	4 (10.3)	17 (43.6)	15 (38.5)
Nerve root compression	0 (0.0)	0 (0.0)	7 (63.6)	4 (36.4)
Loss of disc height	2 (7.4)	1 (3.7)	11 (40.7)	13 (48.2)
Radial bulging of disc	9 (18.0)	10 (20.0)	20 (40.0)	11 (22.0)

normal distributions, whereas the non-parametric Wilcoxon signed rank test was used for comparison of the medians of parameters with asymmetric distributions. A p-value of less than 0.05 was defined as denoting a significant difference in comparisons. Statistical analyses and plots were performed with PASW Statistics, version 18.0 (SPSS Inc., Chicago, IL, USA).

## Results

### Changes of radiographic pathologic feature during axial-loaded MRI

Forty-five subjects, 21 males and 24 females, were prospectively examined with both unloaded and axial-loaded MRI and included in this studies. Their median age was 37.7 (minimum 21.6, maximum 71.5) years, and average body mass index (BMI) was  $25.3 \pm 4.7$  kg/m<sup>2</sup>. The frequency of change of radiographic feature during axial-loaded MRI compared with that during MRI without loading are presented in Table 1. Change of disc bulging or protrusion (36.5%), spinal canal stenosis (48.9%), narrowing of spinal neural foramina (43.6%), nerve root compression (63.6%), and radial bulging of disc (40%) were most prominent at the L4-L5 level, while loss of DH (48.2%) was observed at the L5-S1 level. As a result, the quantitative statistical analyses focused on the L4-L5 and L5-S1 levels.

### Comparison of radiographic parameters between unloaded and axial-loaded MRIs

The comparisons of radiographic parameters between unloaded and axial-loaded MRIs are presented in Table 2. In addition, scatter plots illustrate comparisons of all radiographic parameters from unloaded supine MRIs (x-axes) and the differences (diff) in the values between axial-loaded and unloaded MRIs (y-axes).

**A) Disc bulging and narrowing of dural sac:** Figure 3 is an example of axial T2W images from the unloaded

MRI (Figure 3A) and axial-loaded MRI (Figure 3B) of the same subject at the L4-L5 level, showing the changes on DA and DCSA associated with axial-loading. Disc protrusion and increased DA (dashed arrows) was observed during axial-loading compared with the findings without loading. Spinal canal stenosis with decrease of DCSA (asterisk), nerve root compression (arrow), and neural foramina narrowing (arrowhead) were more clearly seen in the axial-loaded MRIs.

During the use of the axial-loading device, IVDs were compressed and mean DA values were slightly increased ( $p < 0.001$ ) at both L4-L5 (3.7%) and L5-S1 (3.8%) levels (Table 2). Spinal canals were narrowed and mean DCSA values were decreased ( $p < 0.001$ ) at both L4-L5 (5.9%) and L5-S1 (3.6%) levels (Table 2). Scatter plots confirmed that DAs (Figure 4A, 5A) generally increased with mean differences between axial-loaded and unloaded MRIs of 0.62 cm<sup>2</sup> and 0.59 cm<sup>2</sup>, while DCSA (Figure 4B, 5B) frequently decreased with mean differences of  $-10.9$  mm<sup>2</sup> and  $-7.8$  mm<sup>2</sup>, at L4-L5 and L5-S1 levels, respectively.

**B) Loss of height and radial bulging of lumbar discs:** Figure 6 is an example of sagittal T1W images from unloaded (Figure 6A) and axial-loaded (Figure 6B) MRIs of the same subject. During axial-loading, the authors found loss of height at the L5-S1 level that caused a decrease of DH (arrow), as well as increases of DAP at both L4-L5 and L5-S1 levels (arrow heads).

Due to the compression of IVDs, mean DH was decreased ( $p < 0.001$ ) at both L4-L5 (6.8%) and L5-S1 (7.9%), while mean DAP was slightly increased ( $p < 0.001$ ) at both L4-L5 (3.6%) and L5-S1 (3.4%) levels (Table 2). The scatter plots confirmed that DH (Figure 4C, 5C) frequently decreased with mean differences of  $-0.57$  mm and  $-0.60$  mm, and DAP (Figure 4D, 5D) generally increased with mean differences of 0.13 mm and 0.12 cm, at L4-L5 and L5-S1 levels, respectively.

**C) Spine curvature:** Figure 7 is an example of

**Table 2.** Comparison of radiographic parameters between unloaded and axial-loaded MRIs

Parameters	Unloaded Mean (SD)	Axial-loaded Mean (SD)	Diff <sup>†</sup> Mean (SD)	%Diff <sup>‡</sup>	95% CI	p-value
DA (cm <sup>2</sup> )						
L4-L5	16.95 (2.70)	17.57 (2.85)	0.62 (0.66)	3.66	0.42 to 0.82	<0.001
L5-S1	15.67 (3.20)	16.26 (3.33)	0.59 (0.45)	3.77	0.46 to 0.73	<0.001
DCSA (mm <sup>2</sup> ) <sup>§</sup> ; median (min to max)						
L4-L5	136.5 (38.2 to 334.0)	125.0 (30.1 to 318.0)	-8.05 (-57 to 2)	-5.90	N/A	<0.001
L5-S1	126.0 (37.0 to 380.0)	122.5 (22.0 to 376.0)	-4.50 (-40 to 15)	-3.57	N/A	<0.001
DH (mm)						
L4-L5	8.36 (1.56)	7.78 (1.50)	-0.57 (0.54)	-6.82	-0.74 to -0.41	<0.001
L5-S1	7.64 (1.87)	7.04 (1.63)	-0.60 (0.48)	-7.85	-0.75 to -0.46	<0.001
DAP (cm)						
L4-L5	3.61 (0.39)	3.74 (0.39)	0.13 (0.08)	3.60	0.10 to 0.15	<0.001
L5-S1	3.53 (0.40)	3.65 (0.39)	0.12 (0.09)	3.40	0.09 to 0.15	<0.001
LA (°)	165.7 (4.7)	163.2 (4.8)	-2.29 (1.63)	-1.38	-2.79 to -1.80	<0.001
LL (°)	44.71 (8.91)	43.94 (8.95)	-0.77 (2.14)	-1.72	-1.42 to -0.12	0.022

DA=cross-sectional area of disc; DCSA=cross-sectional area of dural sac; DH=disc height; DAP=antero-posterior distance of disc; LA=L1-L3-L5 angle; LL=lumbar lordosis; CI=confidence interval; SD=standard deviation; N/A=not available

<sup>†</sup> Mean differences are calculated by axial loaded MRI - unloaded MRI, <sup>‡</sup> %Diff are calculated by (diff / unloaded) × 100%, <sup>§</sup> Wilcoxon signed rank test

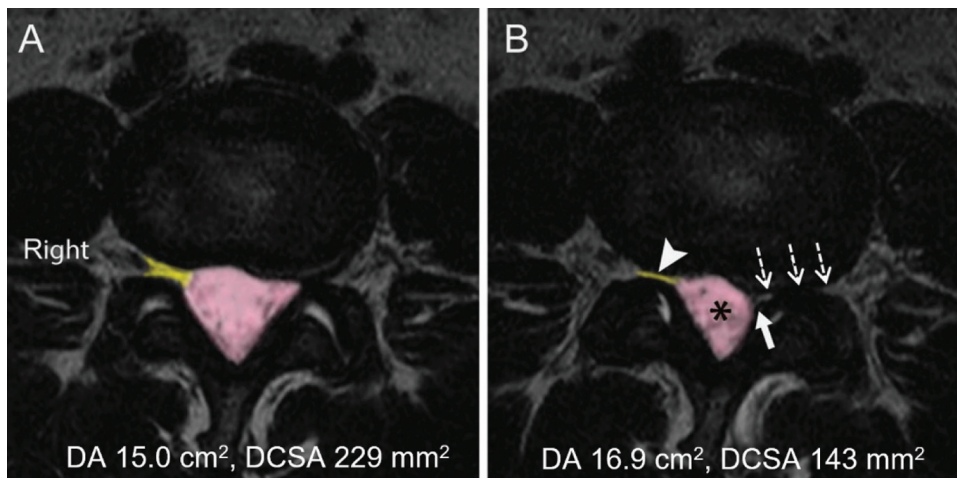


**Figure 3.** MRI examinations of a 36-year-old woman with a 2-year history of low back pain and neurogenic claudication. Axial T2W images at L4-L5 disc level from unloaded (A, L4-L5 DA is 15.0 cm<sup>2</sup> and DCSA is 229 mm<sup>2</sup>) and axial-loaded (B, L4-L5 DA is 16.91 cm<sup>2</sup> and DCSA is 143 mm<sup>2</sup>) MRIs. Note in B the disc bulging with moderate left subarticular-foraminal disc protrusion (dashed arrows) causing left L5 traversing nerve root compression (arrow), changed configuration of the fat pad, and thickening of the ligamenta flava. Also observed are a degree of spinal stenosis increased from mild to moderate degree (asterisk) and narrowing of the right L5 neural foramina (arrow head).

sagittal T1W images from unloaded (Figure 7A) and axial-loaded (Figure 7B) MRIs of the same subject, showing decreases of LA and LL during axial loading.

L1-L3-L5 angle (-1.4%, p<0.001) and lumbar lordosis (-1.7%, p=0.02) were slightly decreased

with small differences of -2.3° and -0.8°, respectively (Table 2). Scatter plots confirmed that LA decreased in all subjects during axial-loading with a maximal decrease of 8.0° (Figure 8A), while only 10 of the 45 subjects had increased LL values with maximal

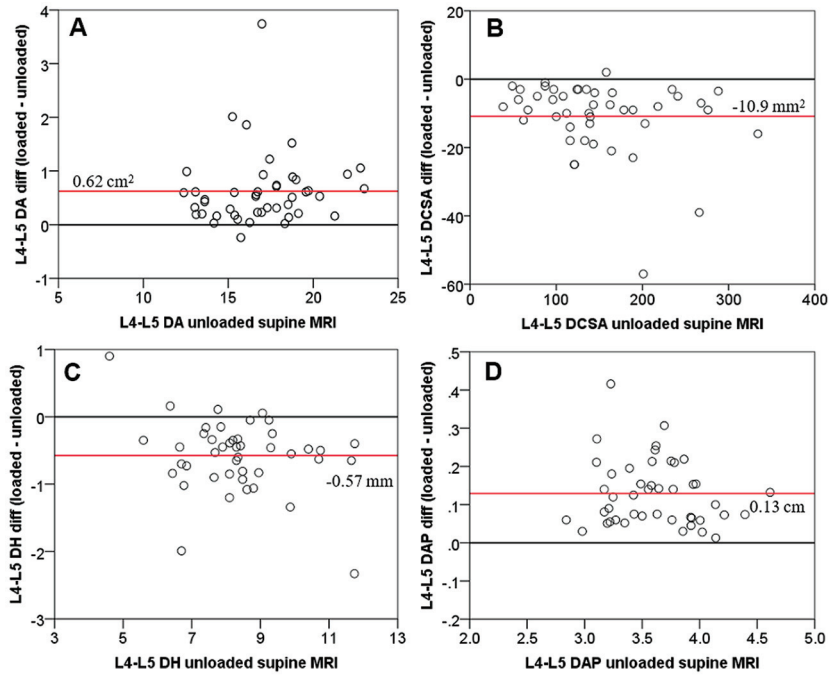


**Figure 4.** Scatter plots of the DA (A), DCSA (B), DH (C), and DAP (D) from unloaded MRIs (x-axes) and the differences (diff) in the values between unloaded and axial-loaded MRIs (y-axes) at the L4-L5 level. The red solid lines indicate the mean differences.

DA=cross-sectional area of disc; DCSA=cross-sectional area of dural sac; DH=disc height; DAP=anterior to posterior diameter of disc

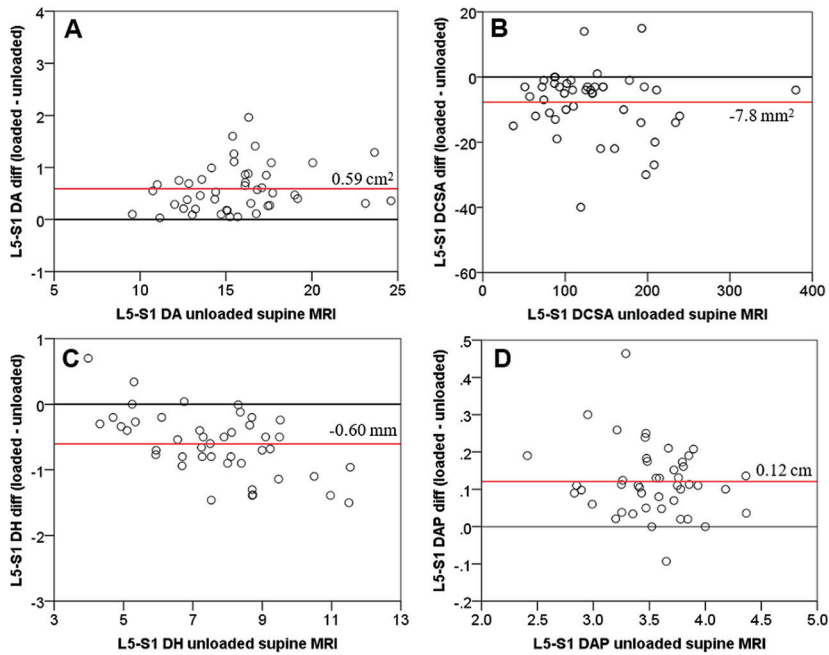


**Figure 5.** Scatter plots of the DA (A), DCSA (B), DH (C), and DAP (D) from unloaded MRIs (x-axes) and the differences (diff) in the values between unloaded and axial-loaded MRIs (y-axes) at the L5-S1 level. The red solid lines indicate the mean differences.

DA=cross-sectional area of disc; DCSA=cross-sectional area of dural sac; DH=disc height; DAP=anterior to posterior distance of disc

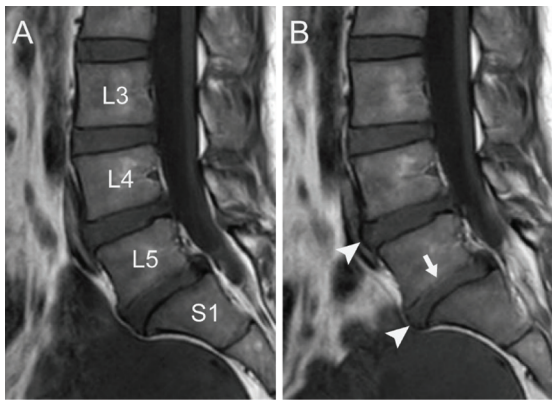


**Figure 6.** MRI examination in a 39-year-old woman with a 3-year history of low back pain. Sagittal T1W images from unloaded (A) and axial-loaded (B) MRIs are shown for comparison. DAPs increased at both L4-L5 (A, 3.23 cm and B, 3.64 cm) and L5-S1 (A, 3.21 cm and B, 3.47 cm) levels (arrow heads).

increase of 6.9° (Figure 8B). The other 35 subjects had decreased LL values with a maximal decrease of 6.6° (Figure 8B).

**Relationship between subject characteristics and changes in radiographic parameters (due to axial loading)**

DA and DAP of the male subjects were greater than those of the female subjects at both L4-L5 ( $p < 0.001$ ) and L5-S1 ( $p < 0.05$ ) levels (Table 3). In addition, DA and DAP values of obese subjects (BMI of 25 or greater) were greater ( $p < 0.05$ ) than those with normal weight (BMI of less than 25) (Table 4). Otherwise, differences in radiographic parameters compared between axial-loaded and unloaded MRIs

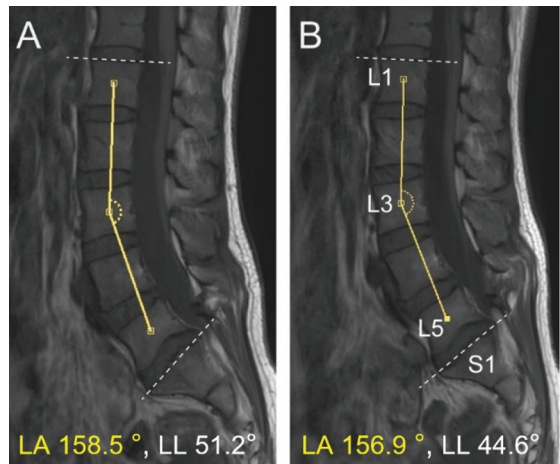


**Figure 7.** MRI examinations of a 38-year-old woman with a 1.5-year history of low back pain and neurogenic claudication. Sagittal T1W images from unloaded (A) and axial-loaded (B) studies are shown for comparison. With axial-loading, LA is slightly decreased (from 158.5° to 156.9°) and LL is decreased (from 51.2° to 44.6°).

were not correlated with subject sex, age nor BMI at the L4-L5 or L5-S1 levels. No additional relationship was found between radiographic parameters and subject characteristics such as sex, age, or BMI, in both unloaded and axial-loaded MRIs.

**Discussion**

In the present study, the radiographic parameters DA, DCSA, DH, distance from anterior to posterior of the IVD, L1-L3-L5 angle, and lumbar lordosis were measured and compared during unloaded and axial-loaded MRIs from 45 subjects with suspected spinal stenosis. The loading was achieved using a

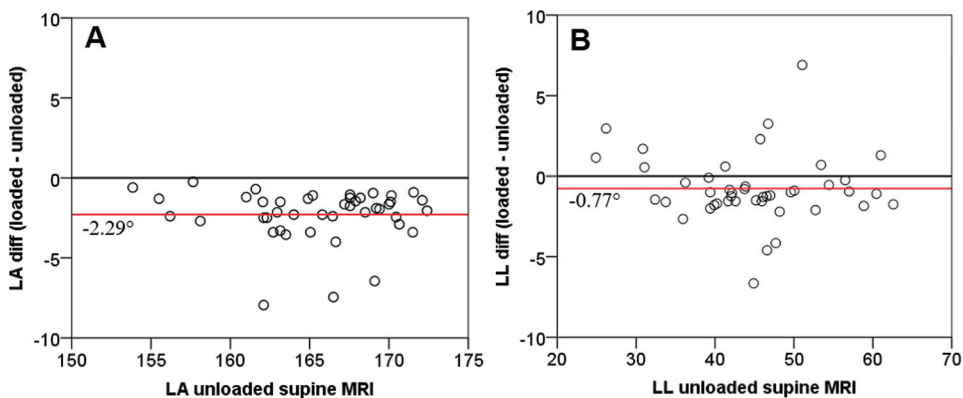


**Figure 8.** Scatter plots of the LA (A) and LL (B) from unloaded MRIs (x-axes) and the differences (diff) in the values from unloaded and axial-loaded MRIs (y-axes). The red solid lines indicate the mean differences.

LA=L1-L3-L5 angle, LL=lumbar lordosis

**Table 3.** Comparison of DA and DAP between males and females at L4-L5 and L5-S1

Level	Parameters	Male (n=21) Mean (SD)	Female (n=24) Mean (SD)	p-value
L4-L5	• DA (cm <sup>2</sup> )			
	Unloaded	18.54 (2.38)	15.55 (2.16)	<0.001
	Axial-loaded	19.30 (2.65)	16.05 (2.25)	<0.001
	• DAP (cm)			
	Unloaded	3.83 (0.37)	3.42 (0.31)	<0.001
	Axial-loaded	3.93 (0.34)	3.57 (0.35)	<0.001
L5-S1	• DA (cm <sup>2</sup> )			
	Unloaded	16.78 (3.28)	14.70 (2.87)	0.028
	Axial-loaded	17.36 (3.41)	15.30 (3.02)	0.038
	• DAP (cm)			
	Unloaded	3.69 (0.34)	3.39 (0.40)	0.011
	Axial-loaded	3.82 (0.33)	3.51 (0.39)	0.008

DA=cross-sectional area of disc; DAP=anterior-posterior distance of disc; SD=standard deviation

SpineMAC lumbosacral spinal compression device made by the authors. Slight differences of 5% or less between the two positions, the non-axial loading and

**Table 4.** Comparison of DA and DAP at L4-L5, grouped as BMI <25 and ≥25

Parameters	BMI <25 (n=25) Mean (SD)	BMI ≥25 (n=20) Mean (SD)	p-value
DA			
Unloaded	16.07 (2.37)	18.19 (2.59)	0.007
Axial-loaded	16.56 (2.46)	18.97 (2.72)	0.004
DAP			
Unloaded	3.50 (0.35)	3.77 (0.38)	0.02
Axial-loaded	3.61 (0.35)	3.91 (0.37)	0.01

DA=cross-sectional area of disc; DAP=anterior-posterior distance of disc; BMI=body mass index; SD=standard deviation

the axial loading were observed for DA at L4-L5 and L5-S1 levels, DCSA at L5-S1, DAP at L4-L5 and L5-S1 levels, LA, and LL. In contrast, the lumbosacral spinal compression device produced major differences of more than 5% to DCSA at L4-L5 and DH at both L4-L5 and L5-S1 levels.

The findings in other studies have been inconsistent (Table 5). Sasani et al<sup>(24)</sup> reported that DCSA values were decreased during axial-load MRIs at both L4-L5 by -10.8% and L5-S1 by -6.7%, as did

**Table 5.** Comparison of studies assessing axial loading on DCSA, DH, and LL

Parameter	Level	Studies	n	Un-loaded Mean	Axial-loaded Mean	Up	%Diff <sup>§</sup> Mean	p-value
DCSA	L4-L5	• Madsen, et al. <sup>(20)</sup>	12, 15**	123	138	136	12.2	NR
		• Sasani, et al. <sup>(24)</sup>	103	138	123	-10.8	NR	
		• Huang, et al. <sup>(25)</sup>	32	108	89	-17.8	NR	
		• Current study <sup>†</sup>	45	137	125	-5.9	<0.01*	
L5-S1	• Madsen, et al. <sup>(20)</sup>	12, 15**	126	132	146	4.8	NR	
	• Sasani, et al. <sup>(24)</sup>	103	134	125	-6.7	NR		
	• Current study <sup>†</sup>	45	126	123	-	-3.6	<0.01*	
DH	L4-L5	• Kimura, et al. <sup>(22)</sup>	8	10.1	9.3	-	-7.9	<0.05*
		• Huang, et al. <sup>(25)</sup>	32	9.0	8.4	-	-7.6	NR
		• Current study	45	8.4	7.8	-	-6.9	<0.01*
	L5-S1	• Kimura, et al. <sup>‡(22)</sup>	8	10.8	10.5	-	-2.7	NS
	• Current study	45	7.6	7.0	-	-7.9	<0.01*	
LL		• Madsen, et al. <sup>(20)</sup>	14, 16**	49.9	49.6	43.9	-0.6	NR
		• Kimura, et al. <sup>(22)</sup>	8	53.4	57.3	-	7.3	NS
		• Huang, et al. <sup>(25)</sup>	32	37.0	39.2	-	5.9	NR
		• Current study	45	44.7	43.9	-	-1.8	<0.01*

DCSA=cross-sectional area of dural sac, DH=disc height, LL=lumbar lordosis, NR=not reported, NS=not statistically significant

\* p<0.05 is statistical significance; \*\* Data are presented as subject numbers during loaded, unloaded studies; † Data presented as median, Wilcoxon signed rank test; ‡ Unpublished data, number estimated from Figure 3 in Kimura et al<sup>(22)</sup>, § %Diff = (loaded - unloaded) / unloaded × 100%



Huang et al<sup>(25)</sup> for DCSA at L4-L5 by -17.8%. The authors findings were in agreement with decreases of the DCSA at both L4-L5 by -5.9% and L5-S1 by -3.6%. However, the present study disagrees with Madsen et al<sup>(20)</sup> that reported that DCSA of axial-loaded MRIs increased 12.2% at L4-L5 and 4.8% at L5-S1 when compared with unloaded MRIs (Table 5). This non-agreement may be due to the difference of patient positioning during scanning. In the study of Madsen et al<sup>(20)</sup>, a cushion was placed below the lower back to induce a slight extension of the lumbar spine, while others<sup>(24,25)</sup> and ourselves did not use such a cushion.

Kimura et al<sup>(22)</sup> reported that a significant decrease ( $p < 0.05$ ) of DH was found only in L4-L5 by -7.9%, while the present study found significant decreases ( $p < 0.01$ ) during axial-load MRIs at both L4-L5 by -6.9% and L5-S1 by -7.9%. Huang et al<sup>(25)</sup> also reported a decrease of DH by -7.6% at L4-L5 but did not report whether the decreases reached significance (Table 5).

Kimura et al<sup>(22)</sup> reported that the lumbar lordosis had a non-significant increase while Huang et al<sup>(25)</sup> only reported an increase when compared with unloaded MRIs (Table 5). The authors found that LA at -1.4% and LL at -1.8% decreased a small but significant amount during axial-loaded MRIs (Table 2). The discrepancy may be due to the supine position during the axial-loaded MRIs. In the present study, the neck was supported by a pillow in the supine position. This may have caused additional straightening of the upper lumbar spine. Madsen et al<sup>(20)</sup> reported that the extent of LL observed with axial-loaded MRIs was slightly decreased by -0.6% when compared with unloaded MRIs. This report agreed with those results. It was shown that placing cushion on the lower back of patients during axial-loaded MRIs, as performed in Madsen et al<sup>(20)</sup>, increases DCSA as well as decreases LL. However, the authors did not know the exact height of the cushion used in their study. Thus, the effects of using cushion support to the lumbar spine during axial-loaded MRIs on IVDs, spinal canal, and spine curvature should be included in future studies. It is worth noting that statistical strength of sample size greater than 20 (Table 5) was studied only by the authors' group and a few others from Sasani et al<sup>(24)</sup> and Huang et al<sup>(25)</sup>.

## Conclusion

Conventional supine MRI is a standard study to assess lumbar spine of patients. However, if the findings do not match the clinically evident

stenotic pattern, the patients should be subjected to a weight bearing MRI either by a lumbosacral spinal compression device or by a standing MRI. The compression device can simulate the effects of weight bearing in supine position when a standing MRI is not available. During axial-loaded MRIs, common pathologic features of lumbar spinal stenosis such as disc bulging, nerve root compression, narrowing of spinal canal, and spinal neural foramina, were observed more frequently than in unloaded supine MRIs. Axial-loaded MRI using a compression device appears superior to supine unloaded MRI for evaluating narrowing of the dural sac and loss of DH, though lumbar lordosis may be underestimated.

## What is already known on this topic?

The effects of axial loading on dural sac, DH, DA, and lumbar lordosis in the previous studies using a commercial device have been inconsistent. In Thailand, a lumbosacral spinal compression device, named SpineMAC, was developed by the authors to simulate weight bearing during supine MRI. There is no study reporting the axial-loading in Thai adults suspected of spinal stenosis using the experimental Spine MAC device.

## What this study adds?

Supine axial-loaded MRI provided more narrowing of dural sac and loss of DH than conventional MRI. Exception was that lumbar lordosis may be underestimated. Changes on radiographic parameters due to axial loading were otherwise not correlated with sex, age, or body mass index.

## Acknowledgement

The authors thank Chulaluk Komontri from the Faculty of Medicine, Siriraj Hospital, for statistical consultation and Arthur Brown, research consultant at the Faculty of Medical Technology, Mahidol University, for English editing. This study is supported by National Research Council of Thailand and Mahidol University.

## Conflicts of interest

The authors declare no conflict of interest.

## References

1. Botwin KP, Gruber RD. Lumbar spinal stenosis: anatomy and pathogenesis. *Phys Med Rehabil Clin N Am* 2003;14:1-15.
2. Moon MS, Kim SS, Sihm JC. Lumbar spinal stenosis – a current view. *Orthop Trauma* 2014;28:396-408.

3. Katz JN, Harris MB. Clinical practice. Lumbar spinal stenosis. *N Engl J Med* 2008;358:818-25.
4. Fujiwara A, An HS, Lim TH, Haughton VM. Morphologic changes in the lumbar intervertebral foramen due to flexion-extension, lateral bending, and axial rotation: an in vitro anatomic and biomechanical study. *Spine (Phila Pa 1976)* 2001;26:876-82.
5. Penning L, Wilmink JT. Biomechanics of lumbosacral dural sac. A study of flexion-extension myelography. *Spine (Phila Pa 1976)* 1981;6:398-408.
6. Takahashi S, Lord EL, Hayashi T, Cohen JR, Lao L, Yao Q, et al. Radiologic factors associated with the dynamic change of dural sac diameter in lumbar spine: a kinematic MRI study. *Clin Spine Surg* 2017;30:E827-32.
7. Amundsen T, Weber H, Lilleås F, Nordal HJ, Abdelnoor M, Magnaes B. Lumbar spinal stenosis. Clinical and radiologic features. *Spine (Phila Pa 1976)* 1995;20:1178-86.
8. Bolender NF, Schönström NS, Spengler DM. Role of computed tomography and myelography in the diagnosis of central spinal stenosis. *J Bone Joint Surg Am* 1985;67:240-6.
9. Wilmink JT, Penning L. Influence of spinal posture on abnormalities demonstrated by lumbar myelography. *AJNR Am J Neuroradiol* 1983;4:656-8.
10. Zander DR, Lander PH. Positionally dependent spinal stenosis: correlation of upright flexion-extension myelography and computed tomographic myelography. *Can Assoc Radiol J* 1998;49:256-61.
11. Kanno H, Endo T, Ozawa H, Koizumi Y, Morozumi N, Itoi E, et al. Axial loading during magnetic resonance imaging in patients with lumbar spinal canal stenosis: does it reproduce the positional change of the dural sac detected by upright myelography? *Spine (Phila Pa 1976)* 2012;37:E985-92.
12. Jordan J, Konstantinou K, O'Dowd J. Herniated lumbar disc. *BMJ Clin Evid* 2011;2011:1118.
13. Inufusa A, An HS, Lim TH, Hasegawa T, Haughton VM, Nowicki BH. Anatomic changes of the spinal canal and intervertebral foramen associated with flexion-extension movement. *Spine (Phila Pa 1976)* 1996;21:2412-20.
14. Danielson B, Willén J. Axially loaded magnetic resonance image of the lumbar spine in asymptomatic individuals. *Spine (Phila Pa 1976)* 2001;26:2601-6.
15. Willén J, Danielson B, Gaulitz A, Niklason T, Schönström N, Hansson T. Dynamic effects on the lumbar spinal canal: axially loaded CT-myelography and MRI in patients with sciatica and/or neurogenic claudication. *Spine (Phila Pa 1976)* 1997;22:2968-76.
16. Danielson BI, Willén J, Gaulitz A, Niklason T, Hansson TH. Axial loading of the spine during CT and MR in patients with suspected lumbar spinal stenosis. *Acta Radiol* 1998;39:604-11.
17. Kanno H, Ozawa H, Koizumi Y, Morozumi N, Aizawa T, Kusakabe T, et al. Dynamic change of dural sac cross-sectional area in axial loaded magnetic resonance imaging correlates with the severity of clinical symptoms in patients with lumbar spinal canal stenosis. *Spine (Phila Pa 1976)* 2012;37:207-13.
18. Willén J, Danielson B. The diagnostic effect from axial loading of the lumbar spine during computed tomography and magnetic resonance imaging in patients with degenerative disorders. *Spine (Phila Pa 1976)* 2001;26:2607-14.
19. Tarantino U, Fanucci E, Iundusi R, Celi M, Altobelli S, Gasbarra E, et al. Lumbar spine MRI in upright position for diagnosing acute and chronic low back pain: statistical analysis of morphological changes. *J Orthop Traumatol* 2013;14:15-22.
20. Madsen R, Jensen TS, Pope M, Sørensen JS, Bendix T. The effect of body position and axial load on spinal canal morphology: an MRI study of central spinal stenosis. *Spine (Phila Pa 1976)* 2008;33:61-7.
21. Ali H, Saleh A. Lumbar spine MRI axial loading in patients with degenerative spine pathologies: Its impact on the Radiological findings and treatment decision. *Egypt J Radiol Nucl Med* 2015;46:1065-9.
22. Kimura S, Steinbach GC, Watenpaugh DE, Hargens AR. Lumbar spine disc height and curvature responses to an axial load generated by a compression device compatible with magnetic resonance imaging. *Spine (Phila Pa 1976)* 2001;26:2596-600.
23. Lorenc T, Palczewski P, Wójcik D, Glinkowski W, Gołębiowski M. Diagnostic benefits of axial-loaded magnetic resonance imaging over recumbent magnetic resonance imaging in obese lower back pain patients. *Spine (Phila Pa 1976)* 2018;43:1146-53.
24. Sasani H, Solmaz B, Sasani M, Vural M, Ozer AF. Diagnostic importance of axial loaded magnetic resonance imaging in patients with suspected lumbar spinal canal stenosis. *World Neurosurg* 2019;127:e69-75.
25. Huang KY, Lin RM, Lee YL, Li JD. Factors affecting disability and physical function in degenerative lumbar spondylolisthesis of L4-5: evaluation with axially loaded MRI. *Eur Spine J* 2009;18:1851-7.